

# Expanding color flux tubes and instabilities

Hirotsugu Fujii

*Institute of physics, University of Tokyo, Komaba, Tokyo, 153-8902, Japan*

Kazunori Itakura

*Institute of Particle and Nuclear Studies, High Energy Accelerator Research  
Organization (KEK), 1-1, Oho, Ibaraki, 305-0801, Japan*

---

## Abstract

We present an analytic study of the physics of the glasma which is a strong classical gluon field created at early stage of high-energy heavy-ion collisions. Our analysis is based on the picture that the glasma just after the collision is made of color electric and magnetic flux tubes extending in the longitudinal direction with their diameters of the order of  $1/Q_s$  ( $Q_s$  is the saturation scale of the colliding nuclei). We find that both the electric and magnetic flux tubes expand outwards and the field strength inside the flux tube decays rapidly in time. Next we investigate whether there exist instabilities against small rapidity-dependent perturbations for a fixed color configuration. We find that the magnetic background field exhibits an instability induced by the fluctuations in the lowest Landau level, and it grows exponentially in the time scale of  $1/Q_s$ . For the electric background field we find no apparent instability while the possible relation to the Schwinger mechanism for particle pair creations is suggested.

---

## 1 Introduction

There is a missing link in our current understanding of the event evolution in ultra-relativistic heavy-ion collisions. Before the collision, the projectile nuclei at very high energies are described in the framework of the Color Glass Condensate (CGC) [1]. Once the quark-gluon plasma (QGP) is formed in local thermal equilibrium, its time evolution may be described with hydrodynamics [2]. Obviously here it is a big theoretical challenge how the local equilibrium state is established from the non-equilibrium initial condition given by the CGC. In particular, ideal hydrodynamic simulations seem to require that, at

RHIC, thermalization should be realized within a very short period  $\tau < 1$  fm/c, which was a surprise from the viewpoint of the standard theoretical estimates.

Theoretical efforts involve the detailed analyses of the plasma instability (in particular, the Weibel instability) [3] which takes place when the hard particles having very anisotropic distribution in the momentum space interact with soft gauge fields (See Ref. [4] for other scenarios and more references). Although many new interesting phenomena are found in these studies, they are based on the kinetic equation applicable for  $\tau \gtrsim 1/Q_s$  when individual particles are formed out of fields. The plasma instability scenario, therefore, should be carefully examined at the earliest stages  $\tau \lesssim 1/Q_s$ , where the system is so dense that the field description may be more appropriate. In fact, it has been shown that the Boltzmann description is equivalent to the description based on the classical field equations when the occupation number of particles is large [5]. Therefore, it is very likely that the plasma instability scenario can be also applicable even for  $\tau \lesssim 1/Q_s$  where the kinetic theory should be turned over to the classical Yang-Mills equation.

The dense pre-equilibrium system appearing between the first impact and the equilibrated QGP is recently named *Glasma* [6]. The glasma shares some properties with the CGC initial condition. It is still well-described by strong coherent Yang-Mills field, which can be treated as a weak-coupling system. However, unique to the glasma is that it has strong time dependence which is believed to lead eventually to the QGP.

If there are unstable modes in the glasma, it will help the matter evolve to an isotropic/thermalized state more rapidly. In fact, instability in the glasma is already found in the lattice numerical simulation [7]. Properties of the unstable glasma turned out to be similar to those of the Weibel instability in expanding geometry [8] (see also Ref. [9] for more recent results). On the other hand, the instability in the glasma is analytically less understood although there are several works about the initial fluctuation of the glasma [10] and its possible instability [11,12,13,14,15]. In this paper, we shall present a detailed analytic study of the dynamics and instability of the glasma.

Our theoretical framework is based on the following picture. First of all, we look for instabilities of the glasma in a single event to which one fixed color configuration is assigned from the initial distribution of the CGC. Namely we presume that thermal equilibrium should be achieved for each event without taking the average over the distribution of the initial condition. The typical initial configuration specified by the CGC is dense color charges randomly populated on the two-dimensional transverse plane with its coherence length given by  $1/Q_s$ . After the collision, this configuration induces strong electric and magnetic fields in the longitudinal direction  $gE^z \sim gB^z \sim Q_s^2$ , while the

transverse components are vanishing  $E^i = B^i = 0$ . Therefore, the glasma just after the collision can be characterized by flux tubes of strong color fields extending in the longitudinal direction with their transverse size being  $1/Q_s$ . This configuration is independent of the rapidity coordinate, provided that the glasma is expanding longitudinally at the speed of light. We will investigate the time evolution of this flux-tube configuration. Notice that this boost-invariant glasma cannot thermalize because it does not allow longitudinal momentum. It is necessary to introduce the rapidity dependence to the glasma, which is only possible through rapidity-dependent fluctuations. We will analytically examine the stability of the rapidity-dependent fluctuations, and find indeed that there exists an instability in the magnetic background.<sup>1</sup>

The present paper is organized as follows: In the next section, we will define more precisely our theoretical framework, and discuss the properties of boost-invariant glasma as a collection of longitudinal flux tubes. Then, in Sect. 3, we will show a detailed analysis of the rapidity-dependent fluctuations in the boost-invariant background. Summary and discussion will follow in the last section.

## 2 Dynamics of the boost-invariant glasma

At high energies, heavy-ion collisions can be viewed as the CGC-CGC collisions [17]. Namely, the incident nuclei, right-moving 1 and left-moving 2, are highly Lorentz contracted and the valence and large- $x$  degrees of freedom of each nucleus can be represented as static color source,  $\rho_{1,2}(x_\perp)$ , which has random distribution on the transverse plane. The small- $x$  gluons are treated as the radiation field generated by these color charges. Thus, the collision is described by the Yang-Mills equation  $[D_\mu, F^{\mu\nu}] = J^\nu$  with the color current  $J^\nu = \delta^{\nu+}\delta(x^-)\rho_1(x_\perp) + \delta^{\nu-}\delta(x^+)\rho_2(x_\perp)$ , where  $x^\pm = (x^0 \pm x^3)/\sqrt{2}$ . Notice that the current  $J^\mu$  is nonzero only on the light-cone axes  $x^\pm = 0$ . Thus, the dynamics of the glasma in the forward light cone  $x^\pm > 0$  (after the collision) is simply described by the source free Yang-Mills equation  $[D_\mu, F^{\mu\nu}] = 0$  with appropriate boundary conditions on the light-cone axes. It is only through this boundary conditions where the information of the colliding CGC's enters. In fact, as we will discuss later, the initial condition supplied by the CGC is quite unique, and greatly affects the dynamics of the glasma.

In order to describe the glasma expanding in the longitudinal direction at the speed of light, it is convenient to introduce the  $\tau$ - $\eta$  coordinates defined by  $\tau = \sqrt{2x^+x^-}$  and  $\eta = \frac{1}{2}\ln(x^+/x^-)$ . In these coordinates, the source free Yang-Mills equation  $[D_\mu, F^{\mu\nu}] = 0$  is rewritten separately for  $\nu = \tau, \eta, i$  as

---

<sup>1</sup> Similar conclusion is recently obtained in Ref. [16] independently of ours.

$$\tau[D_\tau, \frac{1}{\tau}F_{\tau\eta}] - [D_i, F_{i\eta}] = 0, \quad (1)$$

$$[D_\eta, \frac{1}{\tau}F_{\tau\eta}] - [D_i, \tau F_{i\tau}] = 0, \quad (2)$$

$$\frac{1}{\tau}[D_\tau, \tau F_{i\tau}] - \frac{1}{\tau^2}[D_\eta, F_{i\eta}] + [D_j, F_{ji}] = 0. \quad (3)$$

The second equation is the Gauss law constraint, which is obvious if one rewrites it as  $[D_\eta, P^\eta] + [D_i, P^i] = 0$  by using canonical momenta defined by  $P^\eta \equiv \delta(\tau\mathcal{L})/\delta(\partial_\tau A_\eta) = \frac{1}{\tau}F_{\tau\eta}$  and  $P^i \equiv \delta(\tau\mathcal{L})/\delta(\partial_\tau A_i) = -\tau F_{i\tau}$ . When we solve the Yang-Mills equation, we have to check if the solution indeed satisfies the Gauss law.

For later convenience, we show here the definitions of electric and magnetic field strength ( $i, j, k = 1, 2, 3$ ):

$$E^i \equiv F^{i0}, \quad B^i \equiv -\frac{1}{2}\epsilon_{ijk}F^{jk}. \quad (4)$$

Each component is explicitly represented with respect to quantities in the  $\tau$ - $\eta$  coordinates as ( $i = 1, 2$ )

$$E^i = -F_{i\tau} \cosh \eta + \frac{1}{\tau}F_{i\eta} \sinh \eta, \quad (5)$$

$$E^z = \frac{1}{\tau}F_{\tau\eta}, \quad (6)$$

$$B^i = \epsilon_{ij} \left( F_{j\tau} \sinh \eta - \frac{1}{\tau}F_{j\eta} \cosh \eta \right), \quad (7)$$

$$B^z = -F_{12}. \quad (8)$$

In the rest of this section, we discuss the dynamics of the boost-invariant glasma paying attention to the characteristic properties of the CGC initial conditions. All the calculation is done in the Fock-Schwinger gauge  $A_\tau = \frac{1}{\tau}(x^+A^- + x^-A^+) = 0$ .

## 2.1 Boost-invariant glasma

The glasma created in high-energy collisions expands in the longitudinal direction at the speed of light. In an idealized situation, the gauge fields after the collisions are independent of the rapidity coordinate  $\eta$  [17]:

$$A_\eta = \mathcal{A}_\eta = -\tau^2\alpha(\tau, x_\perp), \quad (9)$$

$$A_i = \mathcal{A}_i = \alpha_i(\tau, x_\perp). \quad (10)$$

We use calligraphic letters to represent boost invariant glasma which corresponds to the classical background fields for instability problem discussed in the next section. These fields satisfy the following equations

$$\frac{1}{\tau^3} \partial_\tau (\tau^3 \partial_\tau \alpha) - [\mathcal{D}_i, [\mathcal{D}_i, \alpha]] = 0, \quad (11)$$

$$\frac{1}{\tau} [\mathcal{D}_i, \partial_\tau \alpha_i] - ig\tau [\alpha, \partial_\tau \alpha] = 0, \quad (12)$$

$$\frac{1}{\tau} \partial_\tau (\tau \partial_\tau \alpha_i) - ig\tau^2 [\alpha, [\mathcal{D}_i, \alpha]] - [\mathcal{D}_j, \mathcal{F}_{ji}] = 0, \quad (13)$$

where the covariant derivative  $\mathcal{D}_i$  and the field strength  $\mathcal{F}_{ji}$  are, respectively, given by  $[\mathcal{D}_i, \alpha] = \partial_i \alpha - ig[\alpha_i, \alpha]$  and  $\mathcal{F}_{ji} = \partial_j \alpha_i - \partial_i \alpha_j - ig[\alpha_j, \alpha_i]$ .

These equations are to be solved with the following initial condition

$$\alpha(\tau = 0, x_\perp) = -\frac{ig}{2} [\alpha_1^i(x_\perp), \alpha_2^i(x_\perp)], \quad (14)$$

$$\alpha^i(\tau = 0, x_\perp) = \alpha_1^i(x_\perp) + \alpha_2^i(x_\perp), \quad (15)$$

where  $\alpha_1^i(x_\perp)$  and  $\alpha_2^i(x_\perp)$  are the classical gauge fields of colliding nuclei, 1 and 2, before the collision. Those are associated with the random color sources on  $x^\pm = 0$ , and therefore the initial fields  $\alpha(\tau = 0, x_\perp)$  and  $\alpha_i(\tau = 0, x_\perp)$ , too, may be considered as random variables. In the original McLerran-Venugopalan model, the color charge distribution on the transverse plane is Gaussian random and there is no correlation between the charges at different transverse points. However, in reality, the charge distribution is not completely random. There is some structure in it. For example, it must be color neutral if it is averaged over the transverse area comparable with the nucleon radius. In fact, one can show that color neutrality is ensured for the transverse area whose extent is larger than  $1/Q_s$  [18]. In other words, this implies that the classical gauge field is randomly distributed on the transverse plane, but its coherence length is at most of the order of  $1/Q_s$ .

Just after the collision, only the longitudinal components of the electric and magnetic fields are nonzero [19,6]

$$E^z|_{\tau=0^+} = -ig[\alpha_1^i, \alpha_2^i], \quad (16)$$

$$B^z|_{\tau=0^+} = ig\epsilon_{ij}[\alpha_1^i, \alpha_2^j]. \quad (17)$$

Note that these fields are *rapidity independent* as the gauge fields  $\alpha_{1,2}^i(x_\perp)$  of the nuclei are assumed to be rapidity independent. On the other hand, as mentioned above, the coherence length in the transverse plane is  $\sim 1/Q_s$ . Therefore, one finds that the initial configuration of the glasma gauge fields

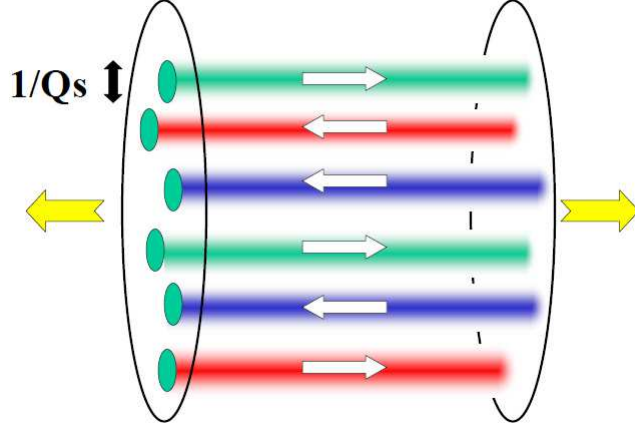


Fig. 1. The color electric and magnetic flux tubes just after the collision. The transverse size of the flux tube is of the order of  $1/Q_s$ .

is represented as collection of color electric and magnetic flux tubes in the longitudinal direction with their diameters of the order of  $1/Q_s$  as shown in Fig. 1. According to the numerical results by Lappi and McLerran [6], these longitudinal fields decay rapidly while the other components are generated as  $\tau$  proceeds.

In the following, for the sake of clarity, we separately discuss two cases with (i)  $\alpha = 0$  and  $\alpha_i \neq 0$ , and with (ii)  $\alpha \neq 0$  and  $\alpha_i = 0$ , which correspond to the magnetic and electric flux tubes, respectively. In fact, the results are valid even when both  $\alpha$  and  $\alpha_i$  are nonzero, provided that they have the same color.

## 2.2 Magnetic flux tube

Let us first consider the dynamics of a magnetic flux tube, which is a unique object in the glasma. We assume that the magnetic flux tube is isolated and there is no longitudinal electric field around it. This is realized by the following

$$\alpha = 0, \quad \alpha_i \neq 0. \quad (18)$$

Then we have the field strengths:

$$E^z = 0, \quad B^z = -F_{12}, \quad E^i = -F_{i\tau} \cosh \eta, \quad B^i = \epsilon^{ij} F_{j\tau} \sinh \eta. \quad (19)$$

Note that the transverse components  $E^i$  and  $B^i$  are transformed among them under the longitudinal boost. We consider the fields only in the local rest-frame ( $\eta = 0$ ), and then  $E^i(\eta = 0) = \partial_\tau \alpha_i$ ,  $B^i(\eta = 0) = 0$ .

For simplicity, we further assume that the magnetic field  $B^z$  is directed to a certain color. This restricts the dynamics to the Abelian subgroup, and one can ignore all the commutators in the equation for  $\alpha_i$ . Since  $\alpha = 0$ , the first Yang-Mills equation (11) is trivial, and the other two equations (12) and (13), respectively, reduce to

$$\partial_\tau k_i \tilde{\alpha}_i = 0, \quad (20)$$

$$\partial_\tau^2 \tilde{\alpha}_i + \frac{1}{\tau} \partial_\tau \tilde{\alpha}_i + k_\perp^2 \left( \delta_{ij} - \frac{k_i k_j}{k_\perp^2} \right) \tilde{\alpha}_j = 0, \quad (21)$$

where we have already introduced the Fourier mode  $\tilde{\alpha}_i(\tau, k_\perp)$  with respect to transverse coordinates. Note that the factor  $(\delta_{ij} - k_i k_j / k_\perp^2)$  is a projection operator to the direction perpendicular to  $k_i$ . Thus, it is convenient to decompose a two-dimensional vector  $\tilde{\alpha}_i$  into two parts (parallel and perpendicular to  $k_i$ )

$$\tilde{\alpha}_i = k_i C_\parallel + \epsilon_{ij} k_j C_\perp. \quad (22)$$

Substituting this into Eq. (20), one finds that  $C_\parallel$  is independent of  $\tau$ . Indeed, this first term is the remaining gauge freedom and unphysical. We set  $C_\parallel = 0$ . Then the Gauss law (20) is automatically satisfied and Eq. (21) becomes a simpler equation for  $C_\perp$ :

$$\partial_\tau^2 C_\perp + \frac{1}{\tau} \partial_\tau C_\perp + k_\perp^2 C_\perp = 0, \quad (23)$$

which is solved by the Bessel function  $J_0(|k_\perp|\tau)$ . Therefore, the solution to Eq. (13) with  $\alpha = 0$  which satisfies the initial condition  $\alpha_i^{\text{init}}(x_\perp)$  is given by

$$\alpha_i(\tau, x_\perp) = \int \frac{d^2 k_\perp}{(2\pi)^2} e^{ik_\perp x_\perp} J_0(|k_\perp|\tau) \tilde{\alpha}_i^{\text{init}}(k_\perp), \quad (24)$$

where the Fourier transform of the initial condition must have the following form

$$\tilde{\alpha}_i^{\text{init}}(k_\perp) \equiv \int d^2 x_\perp e^{-ik_\perp^i x_\perp^i} \alpha_i^{\text{init}}(x_\perp) = \epsilon_{ij} k_j f(k_\perp). \quad (25)$$

Notice that the series expansion of  $J_0(|k_\perp|\tau)$  has only terms with even powers of  $\tau$ . This is consistent with the result of  $\tau$ -expansion developed in Ref. [19]. It is also important to notice that the Bessel function  $J_0(z)$  is an oscillating function with its amplitude decreasing. Hence, the dynamics of the boost-invariant magnetic field is stable if one does not allow for rapidity-dependent fluctuations. The dissipative behavior of the solution is understood as the

effects of longitudinal expansion of the system. If the second term in Eq. (23) were absent, the solution would be simply given by a non-dissipative oscillation  $e^{i|k_\perp|\tau}$ . Thus the dissipative behavior is a result of the second term, which is present due to the  $\tau$ - $\eta$  coordinates that are suitable for describing expanding systems.

To get an intuitive picture of the time dependence of the solution (24), let us discuss a simplest but physically reasonable setting for the initial condition. Consider a single isolated magnetic flux tube which is represented by a Gaussian<sup>2</sup> with its transverse size being  $1/Q_s$ . This can be realized by the following initial condition:

$$\tilde{\alpha}_i^{\text{init}}(k_\perp) \propto -i \frac{\epsilon_{ij} k_j}{k_\perp^2} e^{-\frac{k_\perp^2}{4Q_s^2}}. \quad (26)$$

In fact, one can compute  $B^z$  for  $\tau > 0$  with the result

$$B^z(\tau, r) = B_0 e^{-Q_s^2 r^2} e^{-Q_s^2 \tau^2} I_0(2Q_s^2 r \tau), \quad (27)$$

where  $r = |x_\perp|$  and  $I_0(z)$  is the modified Bessel function. In this expression one can easily check that  $B^z(\tau = 0, r)$  is the Gaussian. Similarly, one can compute the transverse electric field  $E^T \equiv \sqrt{(E^x)^2 + (E^y)^2}$  as

$$E^T(\tau, r) = B_0 e^{-Q_s^2 r^2} e^{-Q_s^2 \tau^2} I_1(2Q_s^2 r \tau). \quad (28)$$

In Fig. 2, we show the transverse profile of  $B^z$  and  $E^T$  at five different instants  $Q_s \tau = 0, 0.5, 1.0, 1.5, 2.0$ . Remarkably, as  $\tau$  increases, the magnetic flux tube expands outwards while the strength inside the flux tube decays rapidly. On the other hand, the transverse component of the electric field is initially zero, but grows until  $Q_s \tau \sim 1$  and then turns to slow decrease.

All these features are intuitively understood by looking at the evolution of the flux tube as a function of  $t = x^0$ , instead of  $\tau$ . In Fig. 3 shown are the lines of the magnetic field in the  $z$ - $x_\perp$  plane at two different instants  $Q_s t = 1$  (solid) and  $Q_s t = 2$  (dashed). The field strengths at  $Q_s z = \pm 1$  ( $\pm 2$ ) for  $Q_s t = 1$  (2) have the Gaussian profile of the initial condition. Non-zero transverse magnetic field appears at  $z \neq 0$ , according to Eq. (19). As the nuclei recede from each other, the flux tube in between is longitudinally stretched out and transversely expands, and thence the field strength decays rapidly in the mid-rapidity region. Notice that this behavior is completely the same as that of

---

<sup>2</sup> We can perform similar analyses for Lorentzian profile  $1/(k_\perp^2 + Q_s^2)$  in the momentum space.



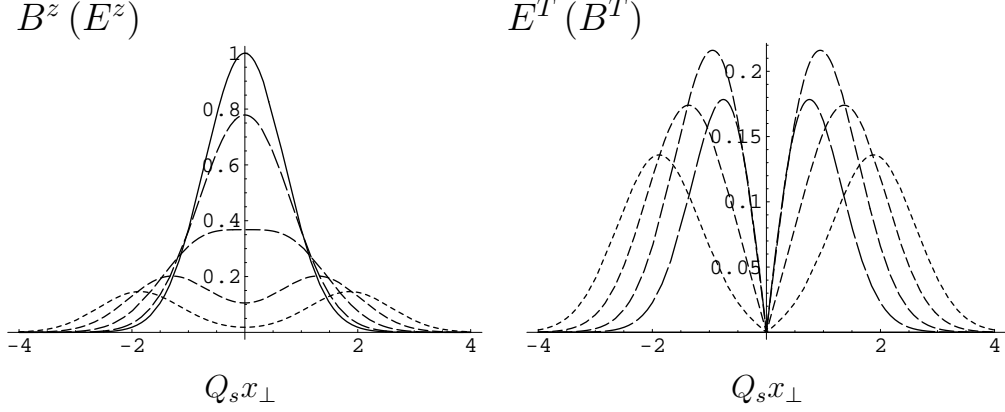


Fig. 2. Spatial profile of the longitudinal electric field  $B^z$  (left) and the transverse magnetic field  $E^T \equiv \sqrt{(E^x)^2 + (E^y)^2}$  (right) at five different times  $Q_s \tau = 0$  (solid), 0.5 (longest dash), 1.0, 1.5, 2.0 (shortest dash). The maximum strength of the electric field is normalized to unity at  $\tau = 0$ , i.e.,  $B_0 = 1$ . Notice that  $E^T = 0$  at  $\tau = 0$ . These are true for  $E^z$  (left) and  $B^T$  (right) of a single electric flux tube.

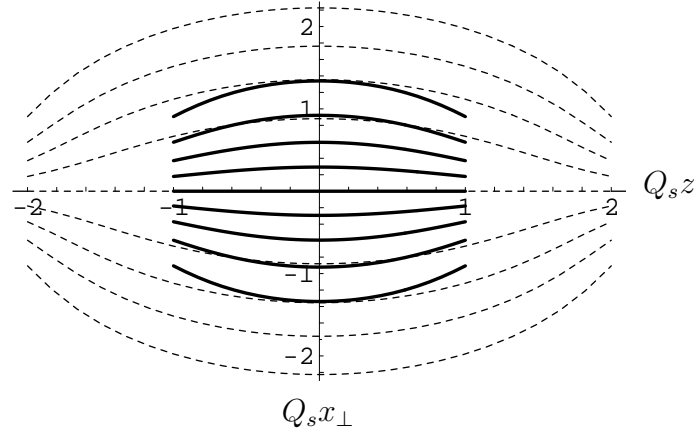


Fig. 3. Lines of the magnetic force at  $Q_s t = 1$  (solid) and 2 (dashed). The sources are located at the longitudinal positions,  $Q_s z = \pm 1$  and  $\pm 2$ , at  $Q_s t = 1$  and 2, respectively. These can be also regarded as the lines of the electric force in the electric flux tube.

ordinary electric field since we have assumed that the gauge field has a single color component.

It is interesting to note that the rapid decay of the longitudinal magnetic field and the slow growth of the transverse electric field is qualitatively similar to the numerical result reported in Ref. [6]. In order to confirm this similarity in a more direct way, let us take the average of  $(B^z)^2$  and  $(E^T)^2$  over the transverse plane. For a single isolated flux tube given by Eq. (39), the integration over the transverse plane gives finite results:

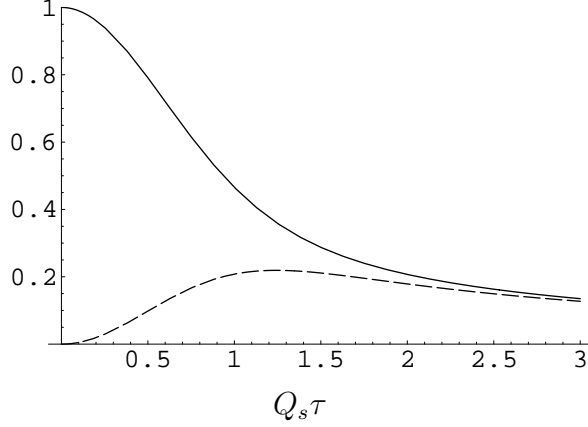


Fig. 4. Time dependence of the magnetic field  $(B^z)^2$  (solid) and the transverse electric field  $(E^T)^2$  (dashed) of a single magnetic flux tube. Both are averaged over the transverse plane, and normalized for  $(B^z)^2$  at  $\tau = 0$ . These are true for  $(E^z)^2$  (solid) and  $(B^T)^2$  (dashed) of a single electric flux tube.

$$\overline{(B^z)^2} \equiv \int d^2x_{\perp} (B^z)^2 = \frac{\pi}{2} \frac{B_0^2}{Q_s^2} e^{-Q_s^2 \tau^2} I_0(Q_s^2 \tau^2), \quad (29)$$

$$\overline{(E^T)^2} \equiv \int d^2x_{\perp} (E^T)^2 = \frac{\pi}{2} \frac{B_0^2}{Q_s^2} e^{-Q_s^2 \tau^2} I_1(Q_s^2 \tau^2). \quad (30)$$

In Fig. 4, we show the time dependence of  $\overline{(B^z)^2}$  and  $\overline{(E^T)^2}$  which is normalized for the magnetic field at  $\tau = 0$ . This is qualitatively very similar to the numerical result of Ref. [6]<sup>3</sup>. For more realistic initial configurations with many flux tubes (of electric and magnetic types), we have to sum up all those contributions. However, if the flux tubes are distributed homogeneously on the transverse plane, which will be realized for the initial condition of well-saturated nuclei, we can expect that the contribution from a single flux tube gives a fair approximation to the actual behavior of  $(B^z)^2$  and  $(E^T)^2$  averaged over the transverse plane. Hence it makes sense (at least qualitatively) to compare our results with the numerical results of Ref. [6].

The large- $\tau$  behavior of  $(B^z)^2$  and  $(E^T)^2$  can be easily determined from the asymptotic form of the modified Bessel function:

$$I_{\nu}(z) \sim \frac{e^z}{\sqrt{2\pi z}}, \quad z \rightarrow \infty. \quad (31)$$

<sup>3</sup> There is no divergence in our computation since we use a Gaussian profile in the transverse plane for the flux tube [14].

Namely, both  $(B^z)^2$  and  $(E^T)^2$  show the same behavior as is evident from the figure:

$$\overline{(B^z)^2} \sim \overline{(E^T)^2} \sim \frac{1}{\tau}. \quad (32)$$

This is consistent with the scaling behavior of the energy density at large  $\tau$ , which is a result of the longitudinal expansion of the system [14]. Indeed, as we will show later for the electric flux tubes, the behavior (32) is common for the longitudinal electric field and transverse magnetic field.

These time dependences of  $\overline{(B^z)^2}$  and  $\overline{(E^T)^2}$  are also understood from the viewpoint of the energy conservation. The problem can be treated just as in the case of the 1-dimensional Bjorken expansion since we have integrated the density over the transverse plane. Change of the energy density per unit rapidity is caused by the  $p dV$  work[20], where  $p$  is the longitudinal pressure and  $dV$  is the volume change  $dV = d\tau$  per unit rapidity for a boost-invariant expanding system. In the magnetic flux tube configuration, the energy density and the longitudinal pressure [7] integrated over  $x_\perp$  are, respectively, given by  $\frac{\tau}{2}[(E^T)^2 + (B^z)^2]$  and  $\frac{1}{2}[(E^T)^2 - (B^z)^2]$  at  $\eta = 0$ . Then the energy conservation implies

$$d\left(\frac{\tau}{2}[(E^T)^2 + (B^z)^2]\right) = -\frac{1}{2}[(E^T)^2 - (B^z)^2] d\tau. \quad (33)$$

As is well known, the energy density per unit rapidity would decrease as  $1/\tau$  without the pressure term. However, for the initial configuration having the longitudinal field alone, the right-hand side is positive [7,6], which slows down the decrease of the energy density. As the transverse field  $\overline{(E^T)^2}$  is generated, the longitudinal pressure is weakened and the behavior of the energy density approaches the  $1/\tau$  dependence.

### 2.3 Electric flux tube

Let us now consider the opposite situation where only a longitudinal electric field is present. This is realized by

$$\alpha \neq 0, \quad \alpha_i = 0. \quad (34)$$

Then, each component of the field strength is given by (at  $\eta = 0$ )

$$E^i = 0, \quad E^z = \frac{1}{\tau} \partial_\tau (-\tau^2 \alpha), \quad (35)$$

$$B^i = \tau \epsilon_{ij} \partial_j \alpha, \quad B^z = 0. \quad (36)$$

We again assume that  $\alpha$  is oriented to a certain color direction which is not necessarily the same one as for  $\alpha^i$  responsible for the magnetic flux tube. While the second and third Yang-Mills equations, (12) and (13), are automatically satisfied under this assumption, the first equation (11) reduces to a very simple differential equation:

$$\frac{1}{\tau^3} \partial_\tau (\tau^3 \partial_\tau \alpha) - \partial_i^2 \alpha = 0. \quad (37)$$

Performing the Fourier transform in the transverse space, one finds that this equation is identical with the Bessel equation. Therefore, the solution satisfying the initial condition  $\alpha(\tau = 0, x_\perp) = \alpha_{\text{init}}(x_\perp)$  is given by

$$\alpha(\tau, x_\perp) = \int \frac{d^2 k_\perp}{(2\pi)^2} e^{i k_\perp x_\perp} \frac{2}{|k_\perp| \tau} J_1(|k_\perp| \tau) \tilde{\alpha}_{\text{init}}(k_\perp), \quad (38)$$

where  $\tilde{\alpha}_{\text{init}}(k_\perp)$  is the Fourier transform of the initial condition  $\alpha_{\text{init}}(x_\perp)$ . One can easily check that this solution satisfies the initial condition by using  $\lim_{\tau \rightarrow 0} \frac{2}{|k_\perp| \tau} J_1(|k_\perp| \tau) = 1$ . Similarly as in the case of the magnetic flux tubes, the expansion of  $J_1(|k_\perp| \tau)/|k_\perp| \tau$  with respect to  $\tau$  gives only even powers of  $\tau$ , which is consistent with the result of  $\tau$ -expansion developed in Ref. [19]. In addition to this, we note that  $J_1(z)/z$  is an oscillating function with its amplitude decreasing. Thus, the dynamics of the boost-invariant background electric field is stable, too.

Let us again consider a simple example in order to understand the time dependence of the solution (38). Consider a single isolated electric flux tube whose transverse size is of the order of  $1/Q_s$ . This can be represented by the initial condition of the Gaussian form:

$$\alpha_{\text{init}}(x_\perp) = \alpha_0 e^{-x_\perp^2 Q_s^2}. \quad (39)$$

Inserting (the Fourier transform of) this into Eq. (38), one finds that the result is represented by infinite series of hypergeometric functions. However, the expressions for the longitudinal electric field  $E^z$  and the transverse magnetic field  $B^T \equiv \sqrt{(B^x)^2 + (B^y)^2}$  become remarkably simple:

$$E^z(\tau, r) = E_0 e^{-Q_s^2 r^2} e^{-Q_s^2 \tau^2} I_0(2Q_s^2 r \tau), \quad (40)$$

$$B^T(\tau, r) = E_0 e^{-Q_s^2 r^2} e^{-Q_s^2 \tau^2} I_1(2Q_s^2 r \tau). \quad (41)$$

Notice that these are the same functional form as  $B^z$  and  $E^T$  in the previous subsection. Thus we can simply replace all the results discussed for  $B^z$  and  $E^T$  by  $E^z$  and  $B^T$ . In particular, Figures 2 and 4 are equally true for  $E^z$  and  $B^T$ , and Figure 3 is true for the electric field.

## 2.4 Coexisting case

So far, we have discussed magnetic and electric flux tubes separately. However, in fact, if both  $\alpha$  and  $\alpha_i$  are oriented to the same direction in the color space, then one can ignore all the commutators in the Yang-Mills equations (11)–(13) yielding decoupled equations for  $\alpha_i$  and  $\alpha$ . Namely, they are given by Eq. (21) and Eq. (37), respectively. Moreover, as is evident from the explicit form of the field strength (5)–(8), the contributions to the field strength from  $\alpha$  and  $\alpha_i$  are additive. Namely, for  $\eta = 0$ , one obtains  $E^i = \partial_\tau \alpha_i$ ,  $E^z = \frac{1}{\tau} \partial_\tau (-\tau^2 \alpha)$ ,  $B^i = \tau \epsilon_{ij} \partial_j \alpha$ , and  $B^z = -\partial_x \alpha_y + \partial_y \alpha_x$ . Therefore, all the results in the previous subsections are valid even in the case where both  $\alpha$  and  $\alpha_i$  are nonzero as far as they have the same color structure.

## 3 Instabilities of the glasma

In the previous section, we have studied the dynamics of boost-invariant glasma as a collection of flux tubes which have typical diameters of  $1/Q_s$  and extend between the two receding nuclei. There we have learned that the flux tubes (longitudinal electric and magnetic fields) expand towards outside in the transverse directions, and the strength inside the tubes rapidly decreases. On the other hand, the transverse components of the field strength  $B^T$  and  $E^T$  are zero at  $\tau = 0$  but grows slowly until around  $Q_s \tau \sim 1$ , where the magnitude of  $B^T$  and  $E^T$  becomes comparable with the longitudinal components  $E^z$  and  $B^z$ . This fact, however, does not imply isotropization of the system. The decay of the longitudinal fields is, in our picture, due to the transverse expansion of the flux tube, which also induces nonzero transverse components of the field strength. Thus, all these can be understood as the *process towards homogeneity in the transverse plane*. In fact, the gauge fields  $\alpha$  and  $\alpha_i$  are still *rapidity independent*. Therefore, thermalization or even isotropization of the system never occurs with this boost-invariant glasma. This is where the rapidity-dependent small fluctuations come into play.

In this section, we discuss the stability of boost-invariant glasma against rapidity-dependent perturbations. The small fluctuations  $a_{i,\eta}$  are defined by

$$A_i = \mathcal{A}_i + a_i(\tau, \eta, x_\perp), \quad A_\eta = \mathcal{A}_\eta + a_\eta(\tau, \eta, x_\perp), \quad (42)$$

where the background fields  $\mathcal{A}_i$  and  $\mathcal{A}_\eta$  are boost-invariant glasma discussed in the previous section (We stay in the Fock-Schwinger gauge  $A_\tau = \mathcal{A}_\tau + a_\tau = 0$ ). The stability of the boost-invariant glasma can be examined by analyzing the Yang-Mills equations (1)–(3) to the linear order in the fluctuations  $a_i$  and  $a_\eta$  on the background fields. The non-Abelian nature uniquely fixes the coupling between the background field and the fluctuations.

In our calculation, to make the situation simple, we approximate the boost-invariant background fields by transversely constant electric or magnetic fields which are of course rapidity independent. This simplification is a reasonable approximation for the fields inside the flux tube. Thus, we implicitly assume that the transverse extent of the constant electric or magnetic field is of the order of  $1/Q_s$  (or slightly larger than that), and we will later examine if the typical transverse size of the unstable mode is smaller than  $1/Q_s$ . In studying the equations for the fluctuations, we restricted ourselves to the  $SU(2)$  color gauge group and greatly benefited from Ref. [21] for technical details.

### 3.1 Fluctuation in the magnetic background field

#### 3.1.1 Constant magnetic field

Consider the simplest case where only time-independent and spatially constant magnetic field is present as the background field. This is a special case of Sect. 2.2 where we treated only  $\alpha_i(\tau, x_\perp)$ . In the following, we consider color  $SU(2)$  group, and assume that the constant magnetic field is directed to the third color component. This is realized by

$$\alpha = 0, \quad \alpha_i^a = \delta^{a3} \frac{B}{2} (y\delta_{i1} - x\delta_{i2}), \quad (43)$$

where  $B(>0)$  is independent of  $\tau$ . The equations for fluctuations are coupled equations for  $a_\eta$  and  $a_i$ , and are still complicated as they are. If one assumes that  $a_\eta \neq 0$  and  $a_i = 0$ , then one can show that  $a_\eta$  is stable. We expect this is true even in the full coupled equations, and we rather consider the opposite case:  $a_\eta = 0$  and  $a_i \neq 0$ . Then the Yang-Mills equations are

$$[\mathcal{D}_i, \partial_\eta a_i] = 0, \quad (44)$$

$$[\mathcal{D}_i, \tau \partial_\tau a_i] = 0, \quad (45)$$

$$-\frac{1}{\tau} \partial_\tau (\tau \partial_\tau a_i) + \frac{1}{\tau^2} \partial_\eta^2 a_i + [\mathcal{D}_j, \delta \mathcal{F}_{ji}] - ig[a_j, \mathcal{F}_{ji}] = 0, \quad (46)$$

where  $\delta\mathcal{F}_{ji} = [\mathcal{D}_j, a_i] - [\mathcal{D}_i, a_j]$ . The  $\eta$  dependence can be easily treated by introducing the Fourier transform. The first equation implies:

$$[\mathcal{D}_i, a_i] = 0. \quad (47)$$

This is the Gauss law. If this is satisfied, the second equation is trivially satisfied, too. The Gauss law is still very helpful in simplifying the third equation. After a long manipulation, we can rewrite the third equation as follows:

$$\begin{aligned} & -\frac{1}{\tau}\partial_\tau(\tau\partial_\tau\tilde{a}_i^a) - \frac{\nu^2}{\tau^2}\tilde{a}_i^a + \partial_\perp^2\tilde{a}_i^a + gB\epsilon^{3ab}\partial_\theta\tilde{a}_i^b \\ & + 2gB\epsilon^{3ab}(\tilde{a}_2^b\delta_{i1} - \tilde{a}_1^b\delta_{i2}) + \frac{g^2B^2r^2}{4}\epsilon^{3cb}\epsilon^{3ba}\tilde{a}_i^c = 0, \end{aligned} \quad (48)$$

where we have introduced the Fourier transform with respect to  $\eta$

$$a_i(\tau, \eta, x_\perp) = \int \frac{d\nu}{2\pi} e^{i\nu\eta} \tilde{a}_i(\tau, \nu, x_\perp), \quad (49)$$

and cylindrical coordinates

$$x = r \cos \theta, \quad y = r \sin \theta. \quad (50)$$

At this stage, it is obvious that the ‘neutral’ fluctuation  $a_i^3$  is stable. The solution of Eq. (48) without the coupling to the constant  $B$ , is given by the Bessel function  $\tilde{a}_i^3 \propto J_{i\nu}(|k_\perp|\tau)$ , which shows a dissipative oscillation.

On the other hand, the other color components are not diagonal, and couples with each other through the magnetic field  $B$ . Physically, these fields behave as ‘charged’ matter coupled to the gauge field, and show cyclotron motion. Thus it is convenient to introduce eigen-states of angular momentum operator in the transverse plane, which is given by the  $\theta$ -derivative:

$$\frac{\partial}{\partial\theta} = x\partial_2 - y\partial_1 \equiv -i\hat{L}. \quad (51)$$

Taking the eigen-states of  $\hat{L}$ , i.e.,  $\tilde{a}_i^a \propto e^{im\theta}$ , we can replace  $\partial_\theta$  by  $im$ . Then we find that the transverse structure is equivalent to the two-dimensional harmonic oscillator. This is clearly seen if we introduce the combined fields for colors

$$\tilde{a}_i^{(\pm)} = \tilde{a}_i^1 \pm i\tilde{a}_i^2, \quad (52)$$

and moreover for the transverse coordinate

$$\tilde{a}_{\pm}^{(\cdot)} = \tilde{a}_1^{(\cdot)} \pm i \tilde{a}_2^{(\cdot)}. \quad (53)$$

Now the equation is diagonal with respect to these fields:

$$\begin{aligned} \frac{1}{\tau} \partial_{\tau} (\tau \partial_{\tau} \tilde{a}_{+}^{(\pm)}) + \left( \frac{\nu^2}{\tau^2} \mp mgB \pm 2gB \right) \tilde{a}_{+}^{(\pm)} + \left( -\partial_{\perp}^2 + \frac{g^2 B^2 r^2}{4} \right) \tilde{a}_{+}^{(\pm)} &= 0, \\ \frac{1}{\tau} \partial_{\tau} (\tau \partial_{\tau} \tilde{a}_{-}^{(\pm)}) + \left( \frac{\nu^2}{\tau^2} \mp mgB \mp 2gB \right) \tilde{a}_{-}^{(\pm)} + \left( -\partial_{\perp}^2 + \frac{g^2 B^2 r^2}{4} \right) \tilde{a}_{-}^{(\pm)} &= 0. \end{aligned}$$

The last terms can be identified with the Hamiltonian of the two-dimensional harmonic oscillator. Therefore, one can replace them by the energy eigenvalues  $E_n a_{\pm}^{(\pm)}$  with  $E_n = (2n + |m| + 1)gB$ . Then we finally obtain the equations of the familiar form:

$$\frac{1}{\tau} \partial_{\tau} (\tau \partial_{\tau} \tilde{a}_{+}^{(\pm)}) + \left( E_n \mp mgB \pm 2gB + \frac{\nu^2}{\tau^2} \right) \tilde{a}_{+}^{(\pm)} = 0, \quad (54)$$

$$\frac{1}{\tau} \partial_{\tau} (\tau \partial_{\tau} \tilde{a}_{-}^{(\pm)}) + \left( E_n \mp mgB \mp 2gB + \frac{\nu^2}{\tau^2} \right) \tilde{a}_{-}^{(\pm)} = 0. \quad (55)$$

These are equations for the Bessel functions. Notice that the sign of  $E_n \mp mgB \pm 2gB$  or  $E_n \mp mgB \mp 2gB$  crucially affects the behavior of the solution. If it is negative, the solution is unstable. For the  $+$  component of the spatial coordinates (Eq. (54)), it can be negative for  $n = 0$ , color  $-$ , and  $m \leq 0$ , i.e.,  $E_0 + mgB - 2gB = -gB$ . On the other hand, for the  $-$  component of the spatial coordinates (Eq. (55)), it can be negative for  $n = 0$ , color  $+$ , and  $m \geq 0$ , i.e.,  $E_0 - mgB - 2gB = -gB$ . Both cases reduce to the same equation which has an unstable solution:

$$\partial_{\tau}^2 f + \frac{1}{\tau} \partial_{\tau} f + \left( -gB + \frac{\nu^2}{\tau^2} \right) f = 0. \quad (56)$$

The solution is given by the modified Bessel function:

$$\tilde{a}_{+}^{(-)}, \tilde{a}_{-}^{(+)} \propto e^{im\theta} r^{|m|} e^{-\frac{gBr^2}{4}} I_{i\nu} \left( \sqrt{gB} \tau \right). \quad (57)$$

These are the exact solutions to the linearized equations for the fluctuation  $a_i(\tau, \eta, x_{\perp})$  in a constant magnetic field. The functional dependence on  $m$  and  $r = |x_{\perp}|$  comes from the wavefunction of the two-dimensional harmonic oscillator with  $n = 0$ . The  $\tau$  dependence is completely determined by the modified Bessel function, which is consistent with the results suggested in



Ref. [14]. By using the asymptotic form (31) of  $I_\nu(z)$  whose leading term is independent of  $\nu$ , we indeed find that the above solution is exponentially divergent:

$$\tilde{a}_+^{(-)}, \tilde{a}_-^{(+)} \sim \frac{e^{\sqrt{gB}\tau}}{\sqrt{2\pi\sqrt{gB}\tau}}. \quad (58)$$

Therefore, instability exists for any  $\nu$  although appearance of the instability depends on  $\nu$ , as we will discuss later. All the other modes except for those mentioned above are stable, and their time dependence is governed by the Bessel function  $J_{i\nu}(\sqrt{gB}\tau)$ .

As we already mentioned, the fluctuations  $\tilde{a}^{(\pm)}$  as the charged matter obey cyclotron motion in a uniform magnetic field. The unstable modes appear in the lowest Landau level ( $n = 0$ ). Interestingly, the fluctuations  $\tilde{a}^{(\pm)}$ , having the opposite sign of charge, show instabilities in the opposite cyclotron rotations to each other. In fact, the existence of instabilities in a constant non-Abelian magnetic field has been known in the ordinary cartesian coordinates [21,22]. What we have done here is essentially to find the same instability phenomena in the  $\tau$ - $\eta$  coordinates (see Ref. [16] for a similar conclusion).

Let us investigate more about the properties of unstable modes. First of all, the smallest spatial size of the instability is given by  $m = 0$ . Namely, the Gaussian profile in the two dimensional plane has the spatial size  $L$  given by

$$L \sim \frac{1}{\sqrt{gB}}. \quad (59)$$

On the other hand, the unstable mode with  $|m| \neq 0$  is distributed in a ring of radius  $\ell \sim \sqrt{2|m|/gB}$ . For the magnetic field created in the CGC,  $gB \sim Q_s^2$ , one finds  $L \sim 1/Q_s$ . Recall that the transverse size of the flux tube is  $\sim 1/Q_s$  at  $\tau = 0$ , but it will expand outward in the transverse plane. Therefore, we conclude that *the magnetic instability (57) will indeed be realized in the time evolution of the glasma.*

Next, we carefully investigate the time evolution of the unstable modes (57) which is completely determined by the modified Bessel function  $I_{i\nu}(z)$ . In Fig. 5, we show typical behaviors of  $\Re\{I_{i\nu}(z)\}$  for two different values of  $\nu$ . The figure indeed shows divergent behavior suggested by the asymptotic form (Eq.(31)). The time scale for the instability to grow is given by

$$\tau_{\text{grow}} \sim \frac{1}{\sqrt{gB}} \sim \frac{1}{Q_s}. \quad (60)$$

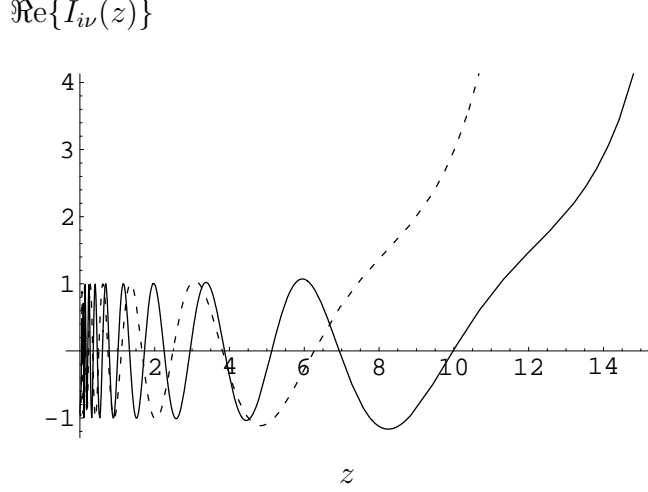


Fig. 5.  $\Re\{I_{i\nu}(z)\}$  for  $\nu = 8$  (dashed) and  $\nu = 12$  (solid) normalized at  $z = 0.1$

However, the time when the instability sets in depends on the value of  $\nu$ , which we denote as  $z_{\text{wait}}$  (because we have to wait until  $z = z_{\text{wait}}$ ). From Fig. 5, one may infer a rough estimate

$$z_{\text{wait}} \sim \nu. \quad (61)$$

This can be indeed justified in two different ways as we discuss below. Consider first the explicit form of  $I_{i\nu}(z)$ :

$$I_{i\nu}(z) = \left(\frac{z}{2}\right)^{i\nu} \sum_{n=0}^{\infty} \frac{(z/2)^{2n}}{n! \Gamma(i\nu + n + 1)}. \quad (62)$$

Notice that the term  $(z/2)^{i\nu} = e^{i\nu \ln z/2}$  simply oscillates for real  $\nu$  and  $z$ , and thus it is not relevant for the instability. One can estimate  $z_{\text{wait}}$  from the other part. Taking the first two terms in the infinite series, one finds

$$I_{i\nu}(z) \sim e^{i\nu \ln \frac{z}{2}} \left\{ \frac{1}{\Gamma(i\nu + 1)} + \frac{(z/2)^2}{\Gamma(i\nu + 2)} \right\} = \frac{e^{i\nu \ln \frac{z}{2}}}{\Gamma(i\nu + 1)} \left\{ 1 + \frac{1 - i\nu}{1 + \nu^2} \left(\frac{z}{2}\right)^2 \right\}.$$

Therefore, one can naively define the position  $z_{\text{wait}}$  where the second term becomes the same order as the first one. For the real part of  $I_{i\nu}(z)$ , this yields

$$\frac{(z_{\text{wait}}/2)^2}{1 + \nu^2} = \kappa^2 \quad (63)$$

for  $\kappa^2 = O(1)$ . Therefore, for large  $\nu$ ,  $z_{\text{wait}}$  grows linearly as a function of  $\nu$ :

$$z_{\text{wait}} = 2\kappa\sqrt{1 + \nu^2} \sim 2\kappa\nu. \quad (64)$$

Choosing  $2\kappa \sim 1$  leads to the rough estimate (61) inferred from Fig. 5.

Another way to estimate  $z_{\text{wait}}$  is based on the differential equation. The modified Bessel function  $I_{i\nu}(\beta z)$  is a solution to  $f'' + f'/z + (-\beta^2 + \nu^2/z^2)f = 0$ . The behavior of the solution changes<sup>4</sup> depending on the sign of the coefficient of the last term  $-\beta^2 + \nu^2/z^2$ . If it is positive, which is realized at small  $z$ , the solution is oscillating. On the other hand, if negative, then unstable. The sign change takes place at  $-\beta^2 + \nu^2/z^2 = 0$ , yielding the same estimate for  $z_{\text{wait}}$ , i.e.,  $z_{\text{wait}} = \nu$  for  $\beta = 1$ .

If we apply this notion to our result, we can estimate the time  $\tau_{\text{wait}}$  when the instability sets in (which may be called “waiting time”). For  $z = \sqrt{gB}\tau \sim Q_s\tau$ ,

$$Q_s\tau_{\text{wait}} \sim \nu. \quad (65)$$

Therefore, for a fixed value of  $\nu$ , the instability will exist only for  $\tau \gtrsim \tau_{\text{wait}}$ . In fact, this waiting time  $Q_s\tau_{\text{wait}}$  can be much longer than the growth time  $Q_s\tau_{\text{grow}} \sim 1$  for large  $\nu$ . Although the instability grows with the characteristic time given by  $\tau_{\text{grow}}$  once it starts, we have to wait until  $\tau_{\text{wait}}$ . Therefore, the total time for the instability to become manifest is estimated as

$$Q_s(\tau_{\text{wait}} + \tau_{\text{grow}}) \sim \nu + 1. \quad (66)$$

It is essentially determined by the waiting time  $\tau_{\text{wait}}$  for large  $\nu$ . But this time scale can be short for small values of  $\nu$ . Since the plasma instability scenario is based on the kinetic approach which is valid only for  $Q_s\tau \gtrsim 1$ , we expect that the *glasma instability* will be more operative for the rapid thermalization of the matter created in the heavy-ion collisions.

The fact that the mode of  $\nu$  has the “waiting time”  $\tau_{\text{wait}}$  for the instability implies that at fixed  $\tau$  there exists a maximum value of  $\nu$  which can participate in the instability, and this maximum value increases with increasing  $\tau$ . In the present case, it is given by

$$\nu_{\text{max}} \sim Q_s\tau. \quad (67)$$

The existence of  $\nu_{\text{max}}$  and its linear dependence on  $\tau$  are consistent with the observation numerically found in Ref. [7]. But the relation between  $\nu_{\text{max}}$  and  $\tau$ , such as the power of  $\tau$  or the coefficient, crucially depends on the behavior of the background field as we will discuss below.

---

<sup>4</sup> We thank A. Iwazaki for this point. Similar argument can be found in Ref. [16].

### 3.1.2 Time-dependent magnetic field

So far, the longitudinal magnetic field was assumed to be time-independent, but the basic equation (48) is in fact true even for time-dependent background field. However, we have to be careful not to replace simply the harmonic oscillator part by its eigenvalues when the magnetic field is time-dependent. This is physically because the cyclotron radius changes in accord with  $B(\tau)$ , which invalidates the factorization of the transverse dynamics from the time dependence. Still, we may assume a situation that the time-dependence of the magnetic field is slow compared with the characteristic time scale of the fluctuation (namely, the growth time of instability), which corresponds to neglecting time derivative of  $B(\tau)$ . Thus we can recover the same equation as before except that the magnetic field  $B$  is replaced by the time-dependent one  $B(\tau)$ . For example, the lowest Landau level yields the following equation

$$\partial_\tau^2 f + \frac{1}{\tau} \partial_\tau f + \left( -gB(\tau) + \frac{\nu^2}{\tau^2} \right) f = 0. \quad (68)$$

This equation can be solved for the following simple case:

$$B(\tau) = B_0 \left( \frac{\tau_0}{\tau} \right)^\gamma. \quad (69)$$

The solution is again given by the modified Bessel function (for  $\gamma = 2$ , the solution does not show rapid growth. It is given by a power of  $\tau$ , or just oscillating):

$$f(\tau) \sim I_{i\beta\nu} \left( \beta \sqrt{gB(\tau)} \tau \right), \quad \beta = \frac{2}{2-\gamma}, \quad \gamma \neq 2. \quad (70)$$

As we mentioned before, the relation between  $\nu_{\max}$  and  $\tau$  depends on the precise form of the background magnetic field:

$$\nu_{\max} \sim \sqrt{gB(\tau)} \tau. \quad (71)$$

Linear dependence appears only for a time-independent magnetic field as seen in Eq. (67).

For the special case of  $\gamma = 1$ , one finds

$$f \sim I_{2i\nu} \left( 2\sqrt{gB_0\tau_0\tau} \right) \quad (72)$$

which is similar to what is expected for an expanding system. On the other hand, if one takes  $\gamma = 1/2$  which is consistent with the asymptotic behavior

(32), the solution is given by

$$f \sim I_{4i\nu/3} \left( \frac{4}{3} \sqrt{gB_0\tau_0^{1/2}} \tau^{3/4} \right), \quad (73)$$

which is consistent with the result of Ref. [16].

For a generic time-dependent magnetic field  $B(\tau)$ , the equation is no longer solved by simple  $I_{i\nu}$ 's but must be solved numerically. Still one can infer the qualitative behavior of the solution from the third term of Eq. (68). Assume that  $B(\tau) > 0$  is slowly decreasing from a certain finite initial value  $B(\tau = 0)$ . Then, the coefficient of the third term  $(-gB(\tau) + \nu^2/\tau^2)$  is positive for small  $\tau$ , but will turn to be negative at a later time. Therefore, the solution is oscillating until  $\tau = \tau_{\text{wait}}$  determined by  $-gB(\tau_{\text{wait}}) + \nu^2/\tau_{\text{wait}}^2 = 0$ , and then starts to grow, which is qualitatively in agreement with the behavior of the modified Bessel function shown in Fig. 5.

Notice that the result (71) for  $\nu_{\text{max}}$  is still valid. In particular, if one substitutes Eq. (29) as the time-dependent magnetic field, one obtains ( $\bar{B} \equiv B_0/2$ )

$$\nu_{\text{max}} \sim \sqrt{g\bar{B}} \left( e^{-Q_s^2\tau^2} I_0(Q_s^2\tau^2) \right)^{1/4} \tau. \quad (74)$$

As the factor  $(e^{-Q_s^2\tau^2} I_0(Q_s^2\tau^2))^{1/4}$  decreases quite slowly, one may observe an approximate linear increase of  $\nu_{\text{max}}$  in  $\tau$ , in accordance with the numerical result [7]. But more precisely, the factor depends on  $\tau$  as  $\sim 1/\tau^{1/4}$ , and thus  $\nu_{\text{max}} \sim \tau^{3/4}$  as already suggested in Eq. (73).

### 3.2 Fluctuation in the electric background field

#### 3.2.1 Constant electric field

Consider the case where only time-independent and spatially constant longitudinal electric field is present as the background field. This is a special case of Sect. 2.3 where we treated only  $\alpha(\tau, x_\perp)$ . Indeed, a constant electric field  $E^z = E$  is realized by the following gauge field:

$$\alpha = -\frac{1}{2}E, \quad \alpha_i = 0. \quad (75)$$

Although the equations for the fluctuations  $a_\eta$  and  $a_i$  in this background are coupled equations, we can simplify them similarly as in the magnetic case. If one assumes that  $a_\eta \neq 0$  and  $a_i = 0$ , then one can show that  $a_\eta$  is stable.

We expect this is true even in the full coupled equations, and we consider the opposite case:  $a_\eta = 0$  and  $a_i \neq 0$ . The Yang-Mills equations are now simplified to the followings:

$$\partial_i[\mathcal{D}_\eta, a_i] = 0, \quad (76)$$

$$\partial_i(\tau \partial_\tau a_i) = 0, \quad (77)$$

$$-\frac{1}{\tau} \partial_\tau(\tau \partial_\tau a_i) + \frac{1}{\tau^2} [\mathcal{D}_\eta, [\mathcal{D}_\eta, a_i]] + \partial_j(\partial_j a_i - \partial_i a_j) = 0. \quad (78)$$

In order to solve these equations, it is convenient to introduce the Fourier transform of  $a_i$  with respect to  $\eta$  and  $x_\perp$

$$a_i(\tau, \eta, x_\perp) = \int \frac{d\nu d^2 k_\perp}{(2\pi)^3} e^{i\nu\eta} e^{ik_\perp x_\perp} \tilde{a}_i(\tau, \nu, k_\perp), \quad (79)$$

and its perpendicular component  $\tilde{b}$  via

$$\tilde{a}_i(\tau, \nu, k_\perp) = \epsilon_{ij} k_j \tilde{b}(\tau, \nu, k_\perp). \quad (80)$$

Then, the third equation can be rewritten as

$$\frac{1}{\tau} \partial_\tau(\tau \partial_\tau \tilde{b}) + k_\perp^2 \tilde{b} + \frac{1}{\tau^2} \left( \nu^2 \tilde{b} - \nu g \tau^2 [E, \tilde{b}] + \frac{g^2 \tau^4}{4} [E, [E, \tilde{b}]] \right) = 0, \quad (81)$$

while the first and second Yang-Mills equations are automatically satisfied by the introduction of  $\tilde{b}$  (because  $k_i \tilde{a}_i = 0$ ).

In order to further simplify the equation, let us consider the  $SU(2)$  case and assume that the electric field is oriented to the third color direction. i.e.,  $E = E^a T^a$  with  $E^1 = E^2 = 0$  and  $E^3 \equiv E$ . Then, one obtains

$$\frac{1}{\tau} \partial_\tau(\tau \partial_\tau \tilde{b}^a) + \frac{1}{\tau^2} \left( \nu^2 \tilde{b}^a - i\nu g E \tau^2 \epsilon^{3ba} \tilde{b}^b + \frac{g^2 E^2 \tau^4}{4} \epsilon^{3ca} \epsilon^{3cb} \tilde{b}^b \right) + k_\perp^2 \tilde{b}^a = 0.$$

For the ‘neutral’ fluctuation  $a = 3$ , the equation does not depend on  $E$ , and the solution is given by the Bessel function  $\tilde{b}^3 \propto J_{i\nu}(|k_\perp|\tau)$ . Therefore, there is no instability in the fluctuation to the third color direction. On the other hand, the equation is not diagonal for  $a = 1, 2$ . One can easily diagonalize it by introducing

$$\tilde{b}^{(\pm)} = \tilde{b}^1 \pm i \tilde{b}^2. \quad (82)$$

Then one finds

$$\left(\partial_\tau^2 + \frac{1}{\tau}\partial_\tau\right)\tilde{b}^{(\pm)} + \left\{k_\perp^2 + \frac{1}{\tau^2}\left(\nu^2 \pm \nu g E \tau^2 + \frac{g^2 E^2}{4}\tau^4\right)\right\}\tilde{b}^{(\pm)} = 0. \quad (83)$$

Let us first ignore the third term in the bracket since it is proportional to  $\tau^4$  and is small enough compared to the other terms at the earliest times. This approximation should be valid for  $\tau$  satisfying

$$\tau \ll \sqrt{\frac{2\nu}{gE}}. \quad (84)$$

For the electric field in the CGC  $gE \sim Q_s^2$ , this condition reads

$$Q_s \tau \ll \sqrt{2\nu}. \quad (85)$$

Within this approximation, one obtains a simple differential equation:

$$\left(\partial_\tau^2 + \frac{1}{\tau}\partial_\tau\right)\tilde{b}^{(\pm)} + \left(k_\perp^2 \pm \nu g E + \frac{\nu^2}{\tau^2}\right)\tilde{b}^{(\pm)} = 0. \quad (86)$$

This is nothing but the equation for the Bessel functions. As we discussed in the magnetic case, the behavior of the solution depends on the sign of  $k_\perp^2 \pm \nu g E$ . If we assume that both  $E$  and  $\nu$  are positive, then, for the plus sign, it is always positive,  $k_\perp^2 + \nu g E > 0$ , and the solution is given by  $\tilde{b}^{(+)} \propto J_{i\nu}(\sqrt{k_\perp^2 + \nu g E} \tau)$ . Therefore, the fluctuation  $\tilde{b}^{(+)}$  is stable. On the other hand, for the minus sign, if  $k_\perp^2 - \nu g E < 0$ , then the solution is given by the modified Bessel function

$$\tilde{b}^{(-)}(\tau, \nu, k_\perp) \propto I_{i\nu}(\sqrt{\nu g E - k_\perp^2} \tau). \quad (87)$$

As has already been seen, the modified Bessel function  $I_{i\nu}(z)$  shows unstable behavior for *large value* of  $z$ , which corresponds to *late time*. We shall check below whether such an instability will indeed manifest itself within the time specified by Eq. (85).

The condition  $k_\perp^2 - \nu g E < 0$  can be regarded as the condition for the existence of unstable fluctuations. In other words, unstable fluctuation has transverse extent  $L \sim 1/k_\perp$  larger than  $1/\sqrt{\nu g E}$ . Recall that the transverse size of the coherent gauge field is of the order of  $1/Q_s$ . Therefore, unstable fluctuations may exist if the transverse extent  $L$  is smaller than  $1/Q_s$ :

$$\frac{1}{Q_s} > \frac{1}{\sqrt{\nu g E}} \sim \frac{1}{\sqrt{\nu} Q_s}. \quad (88)$$

This is satisfied if the momentum  $\nu$  conjugate to rapidity is large:

$$\nu \gtrsim 1. \quad (89)$$

Since the solution is again given by the modified Bessel function  $I_{i\nu}(z)$ , all the properties discussed for the magnetic instability can be applicable to the present case. Notice that both the waiting time  $\tau_{\text{wait}}$  and the growth time  $\tau_{\text{grow}}$  for the instability depend on  $k_{\perp}^2$ , and that the shortest times are realized for  $k_{\perp} = 0$ . Namely, for fixed  $\nu$ , the shortest waiting time and the shortest growth time are, respectively, given by

$$Q_s \tau_{\text{wait}} \sim \sqrt{\nu}, \quad (90)$$

$$Q_s \tau_{\text{grow}} \sim 1/\sqrt{\nu}. \quad (91)$$

If the waiting time  $Q_s \tau_{\text{wait}}$  plus the growth time  $Q_s \tau_{\text{grow}}$  is within the validity region (85), one may be able to conclude the existence of instability. However, this condition reads

$$Q_s(\tau_{\text{wait}} + \tau_{\text{grow}}) \sim \left(1 + \frac{1}{\nu}\right) \sqrt{\nu} \ll \sqrt{2\nu}, \quad (92)$$

which is, unfortunately, not satisfied by any value of  $\nu > 0$ . Therefore, the approximate equation (86) allows for unstable solution, but it shows the instability only outside the region of validity.

Indeed, this means that one cannot ignore the  $E^2$  term in Eq. (83), and then one finds that its solution does not show instability. This is immediately understood if one notices that the second term in the curly bracket can be written as  $(\nu \pm gE\tau^2/2)^2/\tau^2$  which is always non-negative. Thus, the curly bracket in Eq. (83) never becomes negative. On the other hand, the instability in the approximate equation (86) occurs when the corresponding part becomes negative, which is not allowed in the original equation (83). And the upper limit of the time (85) corresponds to the time when  $(\nu - gE\tau^2/2)^2/\tau^2 = 0$ .

In fact, one can write down the explicit form of the solution to the original equation:

$$\tilde{b}^{(\pm)} \propto \frac{1}{\tau} \left\{ c_+ M_{\kappa, \mu} \left( i \frac{gE}{2} \tau^2 \right) + c_- M_{\kappa, -\mu} \left( i \frac{gE}{2} \tau^2 \right) \right\}, \quad (93)$$

where  $M_{\kappa, \mu}(z)$  is the Whittaker function and  $\kappa$  and  $\mu$  are both pure imaginary numbers

$$\kappa = -\frac{i}{2} \left( \frac{k_{\perp}^2}{gE} \pm \nu \right), \quad \mu = i \frac{\nu}{2}. \quad (94)$$



By using the asymptotic form of the Whittaker function, one finds that there is no instability at large  $\tau$ .

What we have done should be essentially equivalent to the Schwinger mechanism. Unlike the creation of massive fermion and anti-fermion pairs, there is no mass gap for the ‘charged’ gluon matter  $\tilde{b}^{(\pm)}$ . Thus any external electric field allows pair creations. In fact, the ‘charged’ fluctuations are accelerated in the electric field, and acquire large longitudinal momentum  $\nu \pm gE\tau^2/2 = \nu \pm g\mathcal{A}_\eta$  [23]. Therefore, even if the fluctuation does not grow in time, it will be infinitely accelerated towards the ends which are moving at the speed of light. This situation may be also called instability as discussed in Ref. [21]. It should be possible to find more explicit correspondence between our case and the Schwinger mechanism, and it will be interesting to also consider the effect of backreaction. We leave such topics for future study.

### 3.2.2 Time-dependent electric field

Let us briefly discuss the case with time-dependent electric field. Although we can in principle treat any time-dependent electric background, we here discuss only the following simple case where we can easily find the solution to the equation:

$$E(\tau) = E_0 \left( \frac{\tau_0}{\tau} \right)^\gamma, \quad \gamma \neq 2. \quad (95)$$

To obtain the differential equation for the fluctuations, one has to replace  $E$  in Eqs. (83) and (86) by  $2E(\tau)/(2 - \gamma) \equiv \beta E(\tau)$  (instead of  $E(\tau)$ ). Then, for the approximate equation (86),

$$\left( \partial_\tau^2 + \frac{1}{\tau} \partial_\tau \right) \tilde{b}^{(\pm)} + \left( k_\perp^2 + \frac{\nu^2}{\tau^2} \pm \beta \nu g E_0 \left( \frac{\tau_0}{\tau} \right)^\gamma \right) \tilde{b}^{(\pm)} = 0. \quad (96)$$

One can reproduce the time-independent case by setting  $\gamma = 0$  ( $\alpha = 1$ ). When  $k_\perp = 0$ , the solution is again given by the modified Bessel function. For example,

$$\tilde{b}^{(-)} \propto I_{i\beta\nu} \left( \sqrt{\beta^3 \nu g E(\tau)} \tau \right). \quad (97)$$

This solution should be a good approximation for small  $\tau$ , but the unstable behavior at large  $\tau$  is just an artifact which appears when we ignore the  $E^2$  term.

## 4 Summary and discussion

We have investigated the dynamics and stability of the glasma based on the picture that the glasma is initially made of longitudinally extending flux tubes with their transverse size being  $1/Q_s$ . For simple Gaussian flux tubes where the longitudinal fields have only one color component, we found that the flux tubes expand outwards as time goes, and the transverse field strengths are accordingly induced. This time evolution is quite consistent with the numerical result reported in Ref. [6], and thus we expect that our simple picture captures the essence of the actual physics situation. It is very remarkable that the Abelian dynamics of the background field in our model reproduces the qualitative behavior of the time-dependence of the energy density found in Ref. [6]. At the same time, this raises a question what is the role of the non-Abelian nature of QCD in the result of Ref. [6]. One of the possible effects of non-Abelian dynamics will be the interactions between flux tubes with different colors. This was ignored in our calculation for an isolated flux tube, but we expect such effects will become relevant only at later time when the overlap between the expanding flux tubes is sizable.

We have studied in detail the response of small rapidity-dependent fluctuations in the background of boost-invariant glasma. Instabilities in the electric or magnetic fields are, if any, expected for the ‘charged’ fluctuations since they can couple to the background field. Recall that there is no preferred color direction in the Yang-Mills theory. Thus, if the field is forced to have only a certain color component, it is quite natural that fluctuations perpendicular to the forced color component (namely, the ‘charged’ fluctuations) become large, and can grow exponentially in some case. In fact, we found that the ‘charged’ fluctuations can grow exponentially only in the magnetic background. On the other hand, the response of the ‘charged’ fluctuations in the electric background is essentially equivalent to the Schwinger mechanism. While the ‘charged’ fluctuation is accelerated infinitely and the system is unstable in the Schwinger mechanism, the fluctuation itself does not grow in time.

The unstable mode in the magnetic background corresponds to the lowest Landau level whose transverse size is  $1/Q_s$ . Thus it can survive in the flux tube which expands in the transverse directions with its initial size being  $1/Q_s$ . The time for the instability to become manifest is estimated as  $Q_s \tau \sim \nu + 1$  where  $\nu$  is the momentum conjugate to the rapidity coordinate. Thus, for small  $\nu$ , instability may occur at very early stage of the collisions, even before the ordinary plasma instability starts to operate. Thus, we hope that the glasma instability play an important role in the early thermalization.

As we have already emphasized, the coupling between the ‘charged’ fluctuation

and the magnetic background field is the essential dynamics for the existence of instability. Since the 'charged' fluctuation itself is the gauge field, such coupling is possible only in the non-Abelian Yang-Mills theories. Therefore, one may say that the glasma instability is a result of non-linearity of the Yang-Mills equation. Having said this, we recall the similarity of the glasma instability with the emergence of chaos in the classical Yang-Mills theory [24]. It is known that the spatially constant Yang-Mills fields exhibit chaos due to the non-linear interactions among the fields. Notice that if there are unstable modes as in the glasma, the Lyapunov exponent for two unstable modes with slightly different initial conditions is given by the growth constant of the unstable modes. This suggests an interesting viewpoint of the Yang-Mills chaos to the glasma instability.

The Weibel instability has been widely studied as the main mechanism of the plasma instability in the context of heavy ion physics [3]. Although it is not evident at present whether the magnetic instability found in the present paper is equivalent to it, our setup is quite similar to that of the plasma instability scenario. For example, the 'hard' particles correspond to the boost-invariant background field in our study, which are supplied by the CGC initial condition, and the 'soft' fields are the rapidity-dependent fluctuations in our study. Since the background field is independent of rapidity, it yields a very anisotropic distribution in the momentum space ( $k_\perp \sim Q_s$ ,  $k_z \sim 0$ ). Moreover, linearizing the Yang-Mills equations for the fluctuations  $a_\mu$ :

$$K^{\mu\nu}[\mathcal{A}]a_\nu = 0, \quad K^{\mu\nu}[\mathcal{A}] = \frac{1}{2} \frac{\delta \mathcal{L}_{\text{YM}}}{\delta A_\mu \delta A_\nu} \Big|_{A_\mu = \mathcal{A}_\mu},$$

is nothing but the computation of the inverse propagator  $K^{\mu\nu}[\mathcal{A}]$  of the 'soft' fields on the background field  $\mathcal{A}_\mu$ . This may correspond to the hard-loop calculation in the study of the plasma instability. We expect that future investigation will clarify the possible relationship between our result and the Weibel instability.

## Acknowledgements

The authors wish to thank Aiichi Iwazaki for discussions and useful correspondences, and Yasuyuki Akiba for urging them to clarify the dynamics of expanding flux tubes. They also thank Kenji Fukushima, François Gelis, Tuomas Lappi and Larry McLerran for their interests, and the YITP International Symposium "*Fundamental Problems in Hot and/or Dense QCD*" during which the present work was finalized. This work is partly supported by Grants-in-Aid (18740169 (KI) and 19540273 (HF)) of MEXT.

## References

- [1] For a recent review, see F. Gelis, T. Lappi and R. Venugopalan, Int. J. Mod. Phys. E **16** (2007) 2595 [arXiv:0708.0047 [hep-ph]].
- [2] For example, U. W. Heinz and P. F. Kolb, “*Two RHIC puzzles: Early thermalization and the HBT problem*,” arXiv: hep-ph/0204061.
- [3] For a recent review, see S. Mrowczynski, PoS C **POD2006** (2006) 042 [arXiv:hep-ph/0611067].
- [4] K. Itakura, Prog. Theor. Phys. Supp. 168 (2007) 295.
- [5] A. H. Mueller and D. T. Son, Phys. Lett. B 582 (2004), 279, T. Stockamp, J. Phys. G **32** (2006) 39 [arXiv:hep-ph/0408206].
- [6] T. Lappi and L. McLerran, Nucl. Phys. A772 (2006) 200.
- [7] P. Romatschke and R. Venugopalan, Phys. Rev. Lett. **96** (2006) 062302 [arXiv:hep-ph/0510121]; Phys. Rev. D **74** (2006) 045011 [arXiv:hep-ph/0605045].
- [8] P. Romatschke and A. Rebhan, Phys. Rev. Lett. **97** (2006) 252301 [arXiv:hep-ph/0605064].
- [9] A. Rebhan, M. Strickland and M. Attems, “*Instabilities of an anisotropically expanding non-Abelian plasma: 1D+3V discretized hard-loop simulations*,” arXiv:0802.1714 [hep-ph].
- [10] K. Fukushima, F. Gelis and L. McLerran, Nucl. Phys. A **786** (2007) 107 [arXiv:hep-ph/0610416].
- [11] S. G. Matinyan, B. Muller and D. H. Rischke, Phys. Rev. C **57** (1998) 1927 [arXiv:nucl-th/9708053].
- [12] D. Kharzeev and K. Tuchin, Nucl. Phys. A **753**, 316 (2005) [arXiv:hep-ph/0501234].
- [13] D. Kharzeev, E. Levin and K. Tuchin, Phys. Rev. C **75**, 044903 (2007) [arXiv:hep-ph/0602063].
- [14] K. Fukushima, Phys. Rev. C **76** (2007) 021902 [Erratum-ibid. C **77** (2007) 029901] [arXiv:0704.3625 [hep-ph]].
- [15] A. Iwazaki, “*Thermalization of Color Gauge Fields in High Energy Heavy Ion Collisions*,” arXiv:0712.1405 [hep-ph].
- [16] A. Iwazaki, “*Decay of Color Gauge Fields in Heavy Ion Collisions and Nielsen-Olesen Instability*,” arXiv:0803.0188 [hep-ph].
- [17] A. Kovner, L. McLerran and H. Weigert, Phys. Rev. D **52** (1995) 6231, *ibid.* Phys. Rev. D **52** (1995) 3809.

- [18] E. Iancu, K. Itakura and L. McLerran, Nucl. Phys. A **724** (2003) 181 [arXiv:hep-ph/0212123].
- [19] R. J. Fries, J. I. Kapusta, and Y. Li, "*Near-Fields and Initial Energy Density in High Energy Nuclear Collisions*", nucl-th/0604054.
- [20] M. Gyulassy and T. Matsui, Phys. Rev. D **29** (1984) 419.
- [21] S. J. Chang and N. Weiss, Phys. Rev. D **20** (1979) 869.
- [22] N. K. Nielsen and P. Olesen, Nucl. Phys. B **144** (1978) 376.
- [23] F. Cooper, J. M. Eisenberg, Y. Kluger, E. Mottola and B. Svetitsky, Phys. Rev. D **48** (1993) 190 [arXiv:hep-ph/9212206].
- [24] T. S. Biro, S. G. Matinyan and B. Muller, "*Chaos and gauge field theory*," World Sci. Lect. Notes Phys. **56** (1994) 1.